JOURNAL OF COMPUTATIONAL PHYSICS **142,** 445–472 (1998)
ARTICLE NO. CP985935

Second-Order Upwinding through a Characteristic Time-Step Matrix for Compressible Flow Calculations

Ying Huang and Alain Lerat

SINUMEF Laboratory, ENSAM, 151, Bd. de l'Hopital, 75013 Paris, France
E-mail: huang@paris.ensam.fr and lerat@paris.ensam.fr

Received June 4, 1997; revised January 13, 1998

An efficient multidimensional scheme is constructed for solving the compressible Euler equations. It is deduced from a centered scheme of the Lax–Wendroff type by using a special time-step in the numerical flux, namely a matricial characteristic time-step. This produces a compact second-order upwinding in a very simple way and leads to accurate non-oscillatory solutions without limiters, entropy correction, or other dissipative correction. The design principle is analysed for hyperbolic systems of conservation laws. It is shown to be close to and less dissipative than a genuinely multidimensional upwinding. Numerical applications are presented for subsonic, transonic, and supersonic aerodynamic problems.

1. INTRODUCTION

Over the past three decades, much progress has been made in the development of efficient multidimensional Euler solvers for compressible flows. However, it is now clear that no numerical method is perfectly suited to all types of flow problems. The design of an optimal method depends on several conditions, such as the Mach number range, the steady or unsteady flow character, and the role of boundary conditions. For instance, for calculating an unsteady flow governed by interactions of fast and strong waves with discontinuities, the most important features for the solver are robustness and good capturing properties of moving strong shocks and contact discontinuities. In classical aerodynamics, the main requirements are not exactly the same. Calculating a steady flow over an airfoil requires a method able to converge quickly towards a steady-state and to give very accurate results around a curved wall.

This work is devoted to the construction of numerical methods for aerodynamic applications, mostly in a steady transonic regime but also in subsonic or low supersonic regimes, with possible extensions to slow unsteady problems, i.e., a problem evolving with a

0021-9991/98 $25.00

characteristic time much greater than the acoustic characteristic time (e.g., flow over an oscillating airfoil). For this type of application, we consider second-order accurate finite-volume methods on structured meshes. Since shock waves are not very strong and are steady or nearly steady, it is possible to construct simple methods involving no flux limitation or artificial viscosity correction and thus no tuning parameter. This means that we look for schemes having an internal numerical dissipation sufficient to ensure stability and avoid spurious oscillations but weak enough to preserve a high accuracy.

Space-centered methods usually require extra dissipation terms. One exception is the implicit centered method proposed by the second author in the early eighties [10, 11, 14, 15]. Using a 3^d point-stencil in d space dimension,[1] this method is based on a kind of Lax–Wendroff approximation and is unconditionally stable and dissipative in the sense of Kreiss. It has been applied to two- and three-dimensional steady transonic flow problems without any correction (see the review paper [12]). Since there is no limiter, the scheme is really second-order accurate. The numerical shock profiles can be sharp and almost non-oscillatory. However, the scheme produces some dependence of the numerical shock structures on the time-step, or more precisely on the CFL number used to reach the steady state. Furthermore, some correction should be applied in unsteady cases to prevent spurious oscillations.

The alternative to centered differencing is upwinding. Upwind methods are generally robust and non-oscillatory and can give CFL independent steady solutions. The basic Roe scheme [20] is almost perfect for 1-D steady flow computation: it is first-order accurate and total-variation diminishing (TVD), but it becomes second-order accurate at steady state and produces shock profiles over one or two mesh cells only. Unfortunately, its straightforward extension to several space-dimensions does not preserve the second-order accuracy at steady-state and spreads the discontinuities inclined with respect to the mesh lines. Several approaches have been proposed to recover the second-order accuracy in most part of the flow, for instance the MUSCL method of Van Leer [23], the anti-diffusive flux addition of Harten [4], or the flux limitation of Sweby [22]. These approaches are accurate, but they introduce some nonlinearities in the scheme, which is not favourable to derive a linearly implicit version with a good convergence to the steady state. Besides, they split the spatial approximation in each space direction. In recent years, many efforts have been done to develop genuinely multidimensional upwind methods. Colella [1] has calculated the numerical fluxes by solving the characteristic form of the full multidimensional equations at the cell faces. A rotated Riemann solver has been proposed in the works of Levy *et al*. [17] and Hirsch *et al*. [6, 7] and some elementary wave models have been studied by Roe [21] and Fey and Jeltsch [3]. The numerical schemes so constructed use no limiter and stay in linear form when applied to a linear hyperbolic problem. They can sharply capture the discontinuities aligned or not with the mesh lines, even though they remain first-order accurate.

The aim of the present paper is to develop a scheme for multidimensional problems that collects together the advantages of the Lerat centered scheme and the Roe upwind scheme. Since the calculation of steady flows is our main concern, we want to avoid the use of limiters or other switch-like ingredients that can prevent the scheme from converging to the steady-state by inducing limiting cycles. The new scheme that we want to construct should satisfy the following properties:

[1] More precisely, the method involves $1 + 2d^2$ points only, that is 3 points for $d = 1$, 9 points for $d = 2$ and 19 points for $d = 3$.

- compactness (at most 3^d points in d dimension)
- truly 2nd order accuracy at steady-state
- no need of limiters for transonic flow problems
- stability and efficiency for large CFL numbers
- numerical steady solutions not depending on the CFL number.

The basic idea relies on the observation that in 1-D the explicit stage of the Lerat scheme, i.e., the classical Lax–Wendroff scheme, can be easily transformed into the Roe scheme by using a special time-step in the numerical flux, namely a matricial characteristic time-step. Since the Roe scheme is an excellent candidate for calculating 1-D steady flows but is difficult to extend to multidimensional problems with a second-order accuracy, we will consider the multidimensional Lerat scheme and modify its time-step for producing an upwinding effect in a simple way. As it will be shown, this can be done by keeping the good features of both schemes, that is, ensuring all the above properties.

The present paper is organized as follows. Section 2 presents the idea of upwinding through the characteristic time-step in one space-dimension. Section 3 discusses the generalization of this idea to scalar two-dimensional problems and analyzes some numerical difficulties. It is notably found that, for the stability reasons, the straightforward extension direction by direction cannot be used. The correct treatment turns out to be quite simple since it comes to use the smallest of two 1-D characteristic time-steps in a Lax–Wendroff formulation. Section 4 shows that this treatment is close to and less dissipative than a genuinely multidimensional upwinding. Section 5 extends the idea to 2-D hyperbolic systems of conservation laws. Then, Section 6 presents the detailed space-approximation together with an implicit time-discretization leading to unconditional linear stability. Finally, numerical applications of the new scheme are presented in Section 7 for two-dimensional subsonic, transonic, and supersonic flow problems.

2. UPWINDING THROUGH A CHARACTERISTIC TIME-STEP IN 1-D

2.1. *Lax–Wendroff and Roe Schemes*

Let us begin with the scalar conservation law,

$$w_t + f(w)_x = 0 \tag{1}$$

and consider difference schemes in conservative form,

$$\Delta w_j = -\sigma\left(h_{j+\frac{1}{2}} - h_{j-\frac{1}{2}}\right), \tag{2}$$

where $w_j = w_j^n$ denotes the numerical solution at time level $t = n\,\Delta t$ and point $x = j\delta x$, σ is the step ratio

$$\sigma = \frac{\Delta t}{\delta x},$$

$h_{j+(1/2)}$ is the numerical flux at $(j + \frac{1}{2})\delta x$ and Δ is the time-difference operator,

$$\Delta w_j = w_j^{n+1} - w_j^n.$$

Introducing also the spatial operators,

$$\begin{aligned}(\delta v)_{j+\frac{1}{2}} &= v_{j+1} - v_j \\ (\mu v)_{j+\frac{1}{2}} &= \frac{1}{2}(v_{j+1} + v_j)\end{aligned} \tag{3}$$

the Lax–Wendroff centered scheme [9] and the Roe upwind scheme [20] can be expressed in form (2) with numerical fluxes respectively defined as

$$h_{j+\frac{1}{2}} = h^{LW}_{j+\frac{1}{2}} = \left(\mu f - \frac{1}{2}\sigma A_R \delta f\right)^n_{j+\frac{1}{2}} \tag{4}$$

$$h_{j+\frac{1}{2}} = h^{R}_{j+\frac{1}{2}} = \left(\mu f - \frac{1}{2}|A_R|\delta w\right)^n_{j+\frac{1}{2}}, \tag{5}$$

where A_R denotes the Roe average of the flux derivative $A = df/dw$, i.e., in the present scalar case,

$$(A_R)_{j+\frac{1}{2}} = \begin{cases} (\delta f)_{j+\frac{1}{2}}/(\delta w)_{j+\frac{1}{2}} & \text{if } \delta w_{j+\frac{1}{2}} \neq 0 \\ A(w_j) & \text{otherwise.} \end{cases}$$

It is well known that the Lax–Wendroff scheme (2), (4) is second-order accurate and may produce spurious oscillations around discontinuities. Its steady solutions satisfy

$$\left(\mu f - \frac{1}{2}\sigma A_R \delta f\right)_{j+\frac{1}{2}} = \text{const.}$$

and thus depend on the time-step or more precisely on the CFL number,

$$\text{CFL} = \max_j \left(\sigma |A_R|_{j+\frac{1}{2}}\right).$$

Spurious oscillations increase as the CFL number decreases and the scheme tends towards the simple centered scheme as the CFL number goes to zero. An efficient way to get rid of these oscillations is to use large CFL numbers. This can be done by adding to the Lax–Wendroff scheme the Lerat implicit stage [10] as

$$\Delta w_j - \frac{1}{2}\sigma^2 \delta\left[A^2_R \delta(\Delta w)\right]_j = -\sigma(\delta h^{LW})_j. \tag{6}$$

Scheme (6) is second-order accurate, always linearly stable, and gives *steady solutions* without oscillations for CFL numbers large enough.

Let us now turn to the Roe scheme (2) and (5). In general, this scheme is first-order accurate, but at steady-state it reduces to

$$\left(\frac{\delta h^R}{\delta x}\right)_j = 0$$

and becomes *second-order accurate*, because the numerical flux (5) can also be written as

$$h^R_{j+\frac{1}{2}} = \left(\mu f - \frac{1}{2}\text{sgn}(A_R)\delta f\right)^n_{j+\frac{1}{2}}$$

so that for any smooth solution of $f(w)_x = 0$, we have

$$\left(\frac{\delta f}{\delta x}\right)_{j+\frac{1}{2}} = (f_x)_{j+\frac{1}{2}} + \mathcal{O}(\delta x^2) = \mathcal{O}(\delta x^2)$$

and

$$\left(\frac{\delta h^R}{\delta x}\right)_j = \left(\frac{\delta \mu f}{\delta x}\right)_j + \mathcal{O}(\delta x^2) = (f_x)_j + \mathcal{O}(\delta x^2).$$

Moreover the exact steady solution is a solution of the Roe scheme in the present 1-D case, but all that does not remain true in several space-dimensions.

The Roe scheme is linearly stable and TVD for CFL ≤ 1. Contrary to the Lax–Wendroff scheme, its steady solution does not depend on the CFL number. Shock profiles are monotonic and spread over one or two mesh cells.

2.2. *Transforming One into the Other*

The Lax–Wendroff scheme can be easily transformed into the Roe scheme by use of a special time-step called the characteristic time-step Δt^c. The latter represents the time necessary for covering the mesh size δx at the characteristic speed A. More precisely, it is defined on the cell face $(j + \frac{1}{2})\,\delta x$ by

$$\Delta t^c_{j+\frac{1}{2}} |A^R|_{j+\frac{1}{2}} = \delta x. \tag{7}$$

By replacing the time-step Δt by $\Delta t^c_{j+(1/2)}$ in the Lax–Wendroff numerical flux (4) but not in the conservative form (2), one gets the modified numerical flux

$$\left(h^{LW}_{j+\frac{1}{2}}\right)^c = \left(\mu f - \frac{1}{2}\sigma^c A_R\, \delta f\right)^n_{j+\frac{1}{2}},$$

where

$$\sigma^c_{j+\frac{1}{2}} = \frac{\Delta t^c_{j+\frac{1}{2}}}{\delta x}.$$

Using (7) the above expression reads

$$\left(h^{LW}_{j+\frac{1}{2}}\right)^c = \left(\mu f - \frac{1}{2}\mathrm{sgn}(A_R)\,\delta f\right)^n_{j+\frac{1}{2}} = h^R_{j+\frac{1}{2}},$$

where sgn denotes the sign function. Thus, in this simple 1-D situation, a second-order centered scheme has been perfectly transformed into an upwind scheme owing to the characteristic time-step and this transformation has *preserved the second-order accuracy at steady-state*.

The idea of a characteristic time-step seems to have been first introduced in 1990 by Powell and Van Leer [19]. The purpose was different since it concerns the speed up of the convergence to the steady-state of an upwind scheme (the characteristic time-step was used in (2), i.e., was applied to the unsteady term). The characteristic time-step has been also

considered by Morton *et al*. [18] for a cell-vertex scheme in one dimension. In the present paper, our aim is to take benefit of the relationship between the Lax–Wendroff and Roe schemes for investigating a simple upwinding technique able to give steady solutions with a second-order accuracy. This follows a first work that we presented at the ECCOMAS'94 Conference [8].

Note that the characteristic time-step definition (7) corresponds to a local CFL number equal to one in the whole mesh. Such a small CFL number could seem to be unfavourable to a fast convergence to the steady-state. This is not the case because the characteristic time-step does not apply on the conservative form (2), i.e., on the discretisation of the unsteady term w_t. It only applies on the time-step involved in the Lax–Wendroff numerical flux. As we will see in Section 6, this allows the development of efficient implicit versions of the method with large (classical) CFL numbers. Obviously, a future improvement of the method could consist in using a second characteristic time-step associated with a large local CFL number for the unsteady term. For the system case, this could be viewed as a kind of preconditioning.

2.3. *Characteristic Time-Step for 1-D Hyperbolic Systems*

Consider now a hyperbolic system of conservation laws in the form (1). The Lax–Wendroff and Roe schemes read as above except that w and $f(w)$ are now vector-valued and the Roe average $(A_R)_{j+(1/2)}$ becomes a matrix (see [20]). Defining the characteristic time-step by the following analogue of (7)

$$\Delta t^c_{j+\frac{1}{2}} |A_R|_{j+\frac{1}{2}} = \delta x I \tag{8}$$

or by

$$\sigma^c_{j+\frac{1}{2}} |A_R|_{j+\frac{1}{2}} = I, \tag{9}$$

where I is an identity matrix, the relationship between both schemes is unchanged, except $\Delta t^c_{j+(1/2)}$ and $\sigma^c_{j+(1/2)}$ are now matrix-valued.

Note that the characteristic time-step matrix is not defined when the Roe average has a zero eigenvalue (for instance at a sonic point), but the useful quantities, that is, the products on the left-hand side of (8) or (9), are still well defined.

3. CHARACTERISTIC TIME-STEP FOR 2-D SCALAR EQUATIONS

3.1. *A Simple Extension Direction by Direction*

For the 2-D scalar equation

$$w_t + f(w)_x + g(w)_y = 0 \tag{10}$$

the Lax–Wendroff time discretization can be written as

$$\frac{\Delta w}{\Delta t} + f(w)_x + g(w)_y = P(w) \tag{11}$$

with

$$P(w) = \frac{1}{2}[\Delta t A(f_x + g_y)]_x + \frac{1}{2}[\Delta t B(f_x + g_y)]_y, \tag{12}$$

where $A = df/dw$ and $B = dg/dw$. The time-step has been inserted inside the brackets to get conservation in case Δt would not be uniform. Space discretization is purely centered.

In addition to ensuring the second-order accuracy in time, the operator P corrects the destabilizing effect of the Euler forward approximation $\Delta w/\Delta t$. To check that the operator P does produce a dissipative effect, we rewrite it as

$$P(w) = \frac{1}{2}[\Delta t(A^2 w_x + AB w_y)]_x + \frac{1}{2}[\Delta t(BA w_x + B^2 w_y)]_y$$

and consider the associated quadratic form

$$\begin{aligned} Q &= \frac{\Delta t}{2}(A^2\xi^2 + 2AB\xi\eta + B^2\eta^2) \\ &= \frac{1}{2}X^t M X \end{aligned}$$

with

$$X = \begin{bmatrix} \xi \\ \eta \end{bmatrix}, \qquad M = \Delta t \begin{bmatrix} A^2 & AB \\ AB & B^2 \end{bmatrix}.$$

Dissipativity in a broad sense of the operator P means that the quadratic form Q is non-negative definite, i.e., the eigenvalues of the symmetric matrix M are positive or null. Here, these eigenvalues are precisely $\Delta t(A^2 + B^2)$ and 0.

The straightforward way to transform the Lax–Wendroff scheme by modifying the time-step in the operator P is to proceed direction by direction, that is, to define two characteristic time-steps similarly as in 1-D:

$$\begin{aligned} \Delta t_1^c|A| &= \delta x \\ \Delta t_2^c|B| &= \delta y. \end{aligned} \tag{13}$$

The semi-discrete expression of the modified scheme stays in form (11) with the new right-hand side,

$$P'(w) = \frac{\delta x}{2}[\mathrm{sgn}(A)(f_x + g_y)]_x + \frac{\delta y}{2}[\mathrm{sgn}(B)(f_x + g_y)]_y.$$

The corresponding quadratic form is

$$Q' = \frac{1}{2}X^t M' X$$

with

$$M' = \begin{bmatrix} \delta x|A| & C \\ C & \delta y|B| \end{bmatrix},$$

where

$$C = \frac{1}{2}\,\mathrm{sgn}(AB)(\delta x|B| + \delta y|A|).$$

Eigenvalues of M' are non-negative if and only if

$$(\delta x|B| - \delta y|A|)^2 \le 0.$$

Therefore the new operator is no longer dissipative, except if

$$\frac{|A|}{\delta x} = \frac{|B|}{\delta y}. \tag{14}$$

This very special case corresponds to an advection along one of the mesh diagonals. In general, the operator P' is not dissipative and it is easy to show that the fully discrete scheme gets unstable.

3.2. *A Better Extension*

First we note that the definition (13) and the condition (14) yield $\Delta t_1^c = \Delta t_2^c$, i.e., the equality of the two characteristic time-steps. Generally speaking, consider the Lax–Wendroff operator P with two arbitrary time-steps Δt_1 and Δt_2, that is,

$$P''(w) = \frac{1}{2}[\Delta t_1 A(f_x + g_y)]_x + \frac{1}{2}[\Delta t_2 B(f_x + g_y)]_y.$$

Dissipativity of P'' is tantamount to

$$[(\Delta t_1 - \Delta t_2)AB]^2 \le 0$$

and thus to $\Delta t_1 = \Delta t_2$. In other words, stable modifications can only be obtained by using a single time-step in the 2-D Lax–Wendroff operator.

To get stability, we now use an unique time-step Δt^c and relax the constraints (13) as

$$\begin{aligned} \Delta t^c|A| &= \delta x \Phi \\ \Delta t^c|B| &= \delta y \Psi. \end{aligned} \tag{15}$$

The operator P in (11) becomes

$$P^c(w) = \frac{\delta x}{2}[\Phi\,\mathrm{sgn}(A)(f_x + g_y)]_x + \frac{\delta y}{2}[\Psi\,\mathrm{sgn}(B)(f_x + g_y)]_y. \tag{16}$$

Let us now determine adequate coefficients Φ and Ψ. First, to define an unique Δt^c from the two relations (15), the following compatibility condition should hold:

$$\frac{|A|}{\delta x}\Psi = \frac{|B|}{\delta y}\Phi. \tag{17}$$

For stability reasons, we require

$$\Phi \ge 0 \qquad \text{and} \qquad \Psi \ge 0. \tag{18}$$

Consider now a one-dimensional problem. When $A \neq 0$ and $B = 0$, condition (17) yields $\Psi = 0$ and the operator (16) reduces to

$$\frac{\delta x}{2}[\Phi|A|w_x]_x.$$

Similarly, when $A = 0$ and $B \neq 0$, the operator becomes

$$\frac{\delta y}{2}[\Psi|B|w_y]_y.$$

Therefore, in order that the scheme reduce to the Roe scheme for 1-D problems, we prescribe

$$(B = 0 \Rightarrow \Phi = 1) \qquad \text{and} \qquad (A = 0 \Rightarrow \Psi = 1). \tag{19}$$

Finally, we look for functions Φ and Ψ that satisfy the constraints (17)–(19) and minimize the distance between the new scheme and the Roe scheme, i.e., minimize the quantity

$$|\Phi - 1| + |\Psi - 1|. \tag{20}$$

This optimization problem is solved by considering Φ and Ψ as functions of the advection direction

$$\Phi = \Phi(\alpha), \qquad \Psi = \Psi(\alpha),$$

where

$$\alpha = \frac{\delta x|B|}{\delta y|A|}. \tag{21}$$

In terms of the parameter α, the constraints (17)–(19) respectively read

$$\begin{aligned} &\Psi(\alpha) = \alpha\Phi(\alpha) \\ &\Phi(\alpha) \geq 0 \\ &\Phi(0) = 1 \qquad \text{and} \qquad \Phi(\alpha) \sim 1/\alpha, \quad \text{as } \alpha \to \infty. \end{aligned} \tag{22}$$

Quantity (20) is optimized for each value of the variable α, i.e., for a given $\alpha > 0$, we look for $z = \Phi(\alpha) \geq 0$ minimizing

$$I(z) = |z - 1| + |\alpha z - 1|.$$

By considering the cases $0 < \alpha \leq 1$ and $\alpha > 1$, the optimal function Φ is found to be

$$\Phi(\alpha) = \begin{cases} 1 & \text{if } 0 < \alpha \leq 1 \\ \frac{1}{\alpha} & \text{if } \alpha > 1. \end{cases}$$

and, consequently

$$\Psi(\alpha) = \begin{cases} \alpha & \text{if } 0 < \alpha \leq 1 \\ 1 & \text{if } \alpha > 1. \end{cases}$$

Let us emphasize that $\alpha < 1$ (resp. $\alpha > 1$) expresses that $|A|/\delta x$ is greater (resp. lower) than $|B|/dy$ i.e., that the advection direction is between the x-direction (resp. y-direction) and a mesh diagonal; in other words, the x-direction (resp. y-direction) is dominant.

Now, observe that the optimal solution can also be written as

$$\begin{aligned} \Phi &= \min\left(1, \frac{1}{\alpha}\right) = \min\left(1, \frac{\delta y|A|}{\delta x|B|}\right) \\ \Psi &= \min(1, \alpha) = \min\left(1, \frac{\delta x|B|}{\delta y|A|}\right) \end{aligned} \tag{23}$$

so that, from (15), it corresponds to

$$\Delta t^c = \min\left(\frac{\delta x}{|A|}, \frac{\delta y}{|B|}\right) = \min\left(\Delta t_1^c, \Delta t_2^c\right). \tag{24}$$

The 2-D characteristic time-step is therefore the *smallest of the two 1-D characteristic time-steps*. It is the time for a particle moving at speed (A, B) to cross a mesh cell starting from a vertex.

4. PRESENT APPROACH COMPARED TO GENUINELY MULTIDIMENSIONAL UPWINDING

It is well known that for many upwind schemes on Cartesian grids, the numerical dissipation is minimal when the advection velocity is parallel to one of the mesh directions.

Consider the linear scalar model

$$w_t + Aw_x + Bw_y = 0, \tag{25}$$

where A and B are two constants. Suppose that the advection velocity norm $C = (A^2+B^2)^{1/2}$ is not null and define a new coordinate system (x', y') by rotating the basic frame with an angle $\theta \in [0, 2\pi)$,

$$\begin{aligned} x' &= x\cos\theta + y\sin\theta \\ y' &= -x\sin\theta + y\cos\theta. \end{aligned} \tag{26}$$

In the new coordinates, Eq. (25) becomes

$$w_t + A'w_{x'} + B'w_{y'} = 0, \tag{27}$$

where

$$\begin{aligned} A' &= A\cos\theta + B\sin\theta \\ B' &= -A\sin\theta + B\cos\theta. \end{aligned}$$

By choosing the angle θ_0 such that

$$\cos\theta_0 = \frac{A}{C} \qquad \text{and} \qquad \sin\theta_0 = \frac{B}{C},$$

Eq. (27) reduces to

$$w_t + C w_{x'} = 0. \tag{28}$$

Let us now apply the Roe scheme to Eq. (28) with a step $\delta x'$. Since $C > 0$, this 1-D scheme can be simply expressed as

$$\frac{\Delta w}{\Delta t} + C w_{x'} = \frac{\delta x'}{2} C w_{x'x'}, \tag{29}$$

where the derivatives should be replaced by centered differences.

For the choice of the step $\delta x'$, we require that it varies continuously between δx (when $B = 0$) and δy (when $A = 0$). Using (26), we take

$$\delta x' = |\cos\theta_0|\delta x + |\sin\theta_0|\delta y. \tag{30}$$

Expressing scheme (29) in the original coordinates (x, y), we have

$$w_{x'} = \cos\theta_0 w_x + \sin\theta_0 w_y = \frac{1}{C}(A w_x + B w_y)$$
$$w_{x'x'} = \frac{1}{C^2}[A(A w_x + B w_y)_x + B(A w_x + B w_y)_y].$$

Therefore, scheme (29) corresponds to

$$\frac{\Delta w}{\Delta x} + A w_x + B w_y = P_0(w), \tag{31}$$

where

$$P_0(w) = \frac{\delta x}{2}[\Phi_0 \operatorname{sgn}(A)(f_x + g_y)]_x + \frac{\delta y}{2}[\Psi_0 \operatorname{sgn}(B)(f_x + g_y)]_y \tag{32}$$

with $f = Aw$, $g = Bw$, and

$$\Phi_0 = \frac{\delta x'}{\delta x}\frac{|A|}{C} = |\cos\theta_0|\left(|\cos\theta_0| + |\sin\theta_0|\frac{\delta y}{\delta x}\right) = \frac{1 + \alpha r^2}{1 + \alpha^2 r^2}$$
$$\Psi_0 = \frac{\delta x'}{\delta y}\frac{|B|}{C} = \alpha\Phi_0,$$

where α is still defined by (21) and r is the mesh aspect-ratio,

$$r = \frac{\delta y}{\delta x}.$$

We observe that the genuinely multidimensional scheme (31)–(32)—in which the space derivatives should be replaced by centered differences—is similar to the scheme (11) and (16) constructed in the previous section from characteristic time-stepping. The only difference lies in the coefficients in the right-hand side. In place of the coefficient pair (Φ, Ψ), we now have (Φ_0, Ψ_0). It turns out that the new coefficients satisfy the three constraints

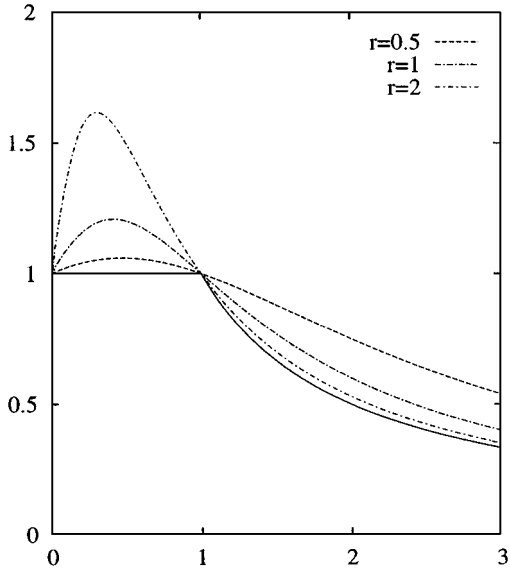

FIG. 1. Coefficients Φ (in full line) and Φ_0 versus the orientation α, for the mesh aspect-ratios $r = 0.5, 1,$ and 2.

(22) prescribed for the old ones and thus are close to them. Furthermore, it is easy to check that

$$\Phi \le \Phi_0, \qquad \Psi \le \Psi_0$$
$$\Phi = \inf_{r \ge 0} \Phi_0, \qquad \Psi = \inf_{r \ge 0} \Psi_0.$$

The coefficient Φ versus the orientation α is shown in Fig. 1 and compared to the coefficient Φ_0 for three values of the step ratio r. Thus, the scheme (11) and (16), deduced from a Lax–Wendroff formulation using a characteristic time-step, is close to and *less dissipative* than the multidimensional upwind scheme (31) and (32). Both schemes are really second-order accurate at steady-state owing to the mixed derivatives in their dissipative operator P or P_0.

5. EXTENSION TO 2-D HYPERBOLIC SYSTEMS

For extending the present approach to a general two-dimensional hyperbolic system of conservation laws, the key point is of course to define the characteristic time-step Δt^c. In one space-dimension, a matricial Δt^c has easily been defined by (8). For a two-dimensional scalar problem, the correct Δt^c is given by (24). Consider now Eq. (10) where the state w and the fluxes $f(w)$ and $g(w)$ in the x- and y-directions are now vector-valued. A simple situation occurs when the flux Jacobian matrices $A(w)$ and $B(w)$ commute. In this case, they can be simultaneously diagonalized and we are brought back to the scalar case. Unfortunately, for the Euler equations, $A(w)$ and $B(w)$ do not commute and the extension is not so direct.

For the general case, we present here an approximate extension that results in an easy implementation. For the sake of simplicity, we choose the matrices Φ and Ψ such that:

(i) the Φ commute with A and Ψ with B,

$$\begin{aligned} \Phi A &= A\Phi \\ \Psi B &= B\Psi \end{aligned} \tag{33}$$

(ii) the eigenvalues of Φ and Ψ are defined by the following simple generalization of (23),

$$\begin{aligned} \lambda_\Phi^{(i)} &= \min\left(1, \frac{\delta y \left|\lambda_A^{(i)}\right|}{\delta x m(B)}\right) \\ \lambda_\Psi^{(i)} &= \min\left(1, \frac{\delta x \left|\lambda_B^{(i)}\right|}{\delta y m(A)}\right), \end{aligned} \tag{34}$$

where $\lambda_A^{(i)}$ denotes the ith eigenvalue of A,

$$m(A) = \min_i \left|\lambda_A^{(i)}\right|$$

and the same for $\lambda_B^{(i)}$ and $m(B)$.

Let also T_A (resp. T_B) be the matrix whose column vectors are the right eigenvectors of A (resp. B), so that

$$\begin{aligned} A &= T_A \Lambda_A T_A^{-1} \\ B &= T_B \Lambda_B T_B^{-1}, \end{aligned}$$

where, for any square matrix M, $\Lambda_M = \mathrm{Diag}[\lambda_M^{(i)}]$. Owing to (33), the matrices Φ and Ψ can be expressed as

$$\begin{aligned} \Phi &= T_A \Lambda_\Phi T_A^{-1} \\ \Psi &= T_B \Lambda_\Psi T_B^{-1}. \end{aligned}$$

The corresponding characteristic time-step matrices are still defined as

$$\begin{aligned} \Delta t_\Phi^c |A| &= \delta x \Phi \\ \Delta t_\Psi^c |B| &= \delta y \Psi \end{aligned}$$

but they are no longer the same. For the first one, we get

$$\Delta t_\Phi^c T_A \Lambda_{|A|} T_A^{-1} = T_A \,\mathrm{Diag}\left[\min\left(\delta x, \frac{\delta y \left|\lambda_A^{(i)}\right|}{m(B)}\right)\right] T_A^{-1}$$

and thus

$$\Delta t_\Phi^c = T_A \,\mathrm{Diag}\left[\min\left(\frac{\delta x}{\left|\lambda_A^{(i)}\right|}, \frac{\delta y}{m(B)}\right)\right] T_A^{-1} \tag{35}$$

which expresses that this time-step matrix has the same eigenvectors as A and its eigenvalues are similar to (24), except that $\delta y/|\lambda_B^{(i)}|$ is replaced by $\delta y/m(B)$, the greatest time-step in the y-direction. Similarly, we obtain

$$\Delta t_\Psi^c = T_B \,\mathrm{Diag}\left[\min\left(\frac{\delta x}{m(A)}, \frac{\delta y}{|\lambda_B^{(i)}|}\right)\right] T_B^{-1}. \tag{36}$$

Expressions (35) and (36) can also be written in the condensed form

$$\begin{aligned} \Delta t_\Phi^c &= \min(\delta x |A^{-1}|, \delta y\, \rho(B^{-1}) I) \\ \Delta t_\Psi^c &= \min(\delta x\, \rho(A^{-1}) I, \delta y |B^{-1}|), \end{aligned} \tag{37}$$

where ρ denotes the spectral radius of a matrix.

In the particular case where $B = 0$ (1-D problem), Δt_Φ^c reduces to the previous characteristic time-step matrix

$$\Delta t_c = \delta x |A|^{-1}.$$

In the 2-D scalar case, from (37) we recover

$$\Delta t_\Phi^c = \Delta t_\Psi^c = \min\left(\frac{\delta x}{|A|}, \frac{\delta y}{|B|}\right).$$

For the practical application to a 2-D hyperbolic system, the method is expressed as

$$\frac{\Delta w}{\Delta t} + f(w)_x + g(w)_y = P^c(w), \tag{38}$$

where the operator P^c is defined by (16), that is,

$$P^c(w) = \frac{\delta x}{2}[\Phi'(f_x + g_y)]_x + \frac{\delta y}{2}[\Psi'(f_x + g_y)]_y, \tag{39}$$

with the coefficient matrices

$$\begin{aligned} \Phi' &= \Phi\, \mathrm{sgn}(A) = T_A \,\mathrm{Diag}\left[\lambda_{\Phi'}^{(i)}\right] T_A^{-1} \\ \Psi' &= \Psi\, \mathrm{sgn}(B) = T_B \,\mathrm{Diag}\left[\lambda_{\Psi'}^{(i)}\right] T_B^{-1}, \end{aligned} \tag{40}$$

where

$$\begin{aligned} \lambda_{\Phi'}^{(i)} &= \mathrm{sgn}\left(\lambda_A^{(i)}\right) \lambda_\Phi^{(i)} \\ \lambda_{\Psi'}^{(i)} &= \mathrm{sgn}\left(\lambda_B^{(i)}\right) \lambda_\Psi^{(i)}. \end{aligned} \tag{41}$$

6. FULLY DISCRETE IMPLICIT SCHEME

Let us now present the fully discrete form of the method, based on a centered approximation of (38)–(41).

6.1. *Explicit Stage*

To ensure stability and dissipation in the sense of Kreiss, we adopt the Lerat formulation of the Lax–Wendroff method (see [12]). It involves a predictor step for each space-direction.

Similarly as in 1-D, we introduce the following discrete operators for a mesh function $v^n_{j,k}$ defined at $t = n\Delta t$, $x = j\delta x$, and $y = k\delta y$ on a Cartesian mesh:

$$\begin{aligned}
\Delta v_{j,k} &= v^{n+1}_{j,k} - v^n_{j,k} \\
(\delta_1 v)_{j+\frac{1}{2},k} &= v^n_{j+1,k} - v^n_{j,k} \\
(\delta_2 v)_{j,k+\frac{1}{2}} &= v^n_{j,k+1} - v^n_{j,k} \\
(\mu_1 v)_{j+\frac{1}{2},k} &= \frac{1}{2}\left(v^n_{j+1,k} + v^n_{j,k}\right) \\
(\mu_2 v)_{j,k+\frac{1}{2}} &= \frac{1}{2}\left(v^n_{j,k+1} + v^n_{j,k}\right).
\end{aligned}$$

The two predictors are defined on the cell interface as

$$\begin{aligned}
(p_1)_{j+\frac{1}{2},k} &= \left(\delta_1 f + \frac{\delta x}{\delta y}\mu_1\delta_2\mu_2 g\right)^n_{j+\frac{1}{2},k} \\
(p_2)_{j,k+\frac{1}{2}} &= \left(\frac{\delta y}{\delta x}\mu_2\delta_1\mu_1 f + \delta_2 g\right)^n_{j,k+\frac{1}{2}}.
\end{aligned} \tag{42}$$

Using these predictors, the method (38)–(41) is discretized as

$$\Delta w_{j,k} = -\Delta t\left(\frac{\delta_1 h_1}{\delta x} + \frac{\delta_2 h_2}{\delta y}\right)_{j,k} \tag{43}$$

with the numerical fluxes

$$\begin{aligned}
(h_1)_{j+\frac{1}{2},k} &= \left(\mu_1 f - \frac{1}{2}\Phi' p_1\right)^n_{j+\frac{1}{2},k} \\
(h_2)_{j,k+\frac{1}{2}} &= \left(\mu_2 g - \frac{1}{2}\Psi' p_2\right)^n_{j,k+\frac{1}{2}},
\end{aligned} \tag{44}$$

where the matrices Φ' and Ψ' are computed from (40)–(41) and (34) using Roe averages at $(j+\frac{1}{2}, k)$ and $(j, k+\frac{1}{2})$.

The above scheme makes use of 9 points only (19 points in 3-D). It is truly *second-order accurate at steady-state*, because for a smooth solution w of

$$f(w)_x + g(w)_y = 0,$$

and $\mathcal{O}(\delta y) = \mathcal{O}(\delta x)$, one obtains

$$(p_1)_{j+\frac{1}{2},k} = \delta x(f_x + g_y)_{j+\frac{1}{2},k} + \mathcal{O}(\delta x^3) = \mathcal{O}(\delta x^3)$$

$$(p_2)_{j,k+\frac{1}{2}} = \delta y(f_x + g_y)_{j,k+\frac{1}{2}} + \mathcal{O}(\delta x^3) = \mathcal{O}(\delta x^3)$$

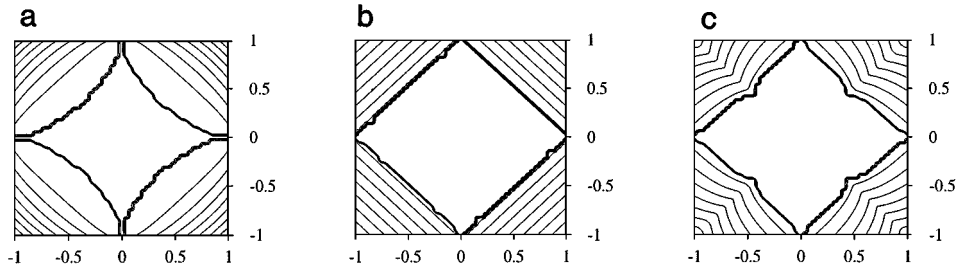

FIG. 2. Stability domains (inside the closed curve in bold line) in terms of $\dot{A} = \frac{\Delta t}{\delta x} A$ and $\dot{B} = \frac{\Delta t}{\delta y} B$. (a) Lax–Wendroff scheme. (b) Roe scheme (1st order). (c) Present explicit scheme.

and, by substitution into (44),

$$\left(\frac{\delta_1 h_1}{\delta x} + \frac{\delta_2 h_2}{\delta y}\right)_{j,k} = \left(\frac{\delta_1 \mu_1 f}{\delta x} + \frac{\delta_2 \mu_2 g}{\delta y}\right)_{j,k} + \mathcal{O}(\delta x^2)$$
$$= (f_x + g_y)_{j,k} + \mathcal{O}(\delta x^2).$$

But, contrary to the original Lax–Wendroff scheme, the numerical steady solution of the present scheme does not depend on the time-step used.

The stability of the present explicit scheme has been studied numerically for a 2-D scalar problem with a constant advection velocity (A, B). Its stability domain is shown in Fig. 2 and compared to those of Lax–Wendroff and Roe schemes. In this figure, the horizontal axis represents $\dot{A} = \frac{\Delta t}{\delta x} A$ and the vertical axis $\dot{B} = \frac{\Delta t}{\delta y} B$. The stability domain of the scheme (43)–(44) is slightly larger than for the Lax–Wendroff scheme and very close to the stability domain of the first-order Roe scheme. It can be approximately expressed by the CFL criterion

$$|\dot{A}| + |\dot{B}| \leq 1,$$

that is,

$$\Delta t \left(\frac{|A|}{\delta x} + \frac{|B|}{\delta y}\right) \leq 1.$$

A sufficient stability condition can also be written as

$$\Delta t \left[\left(\frac{|A|}{\delta x}\right)^2 + \left(\frac{|B|}{\delta y}\right)\right]^{1/2} \leq \frac{\sqrt{2}}{2}.$$

6.2. *Implicit Scheme*

For improving the efficiency of steady-state calculations, we add to the above scheme a suitable implicit stage. By applying the Euler backward time-discretization, we transform the scheme (42)–(44) into

$$\left(\frac{\Delta w}{\Delta t} + \frac{\delta_1 h_1^{n+1}}{\delta x} + \frac{\delta_2 h_2^{n+1}}{\delta y}\right)_{j,k} = 0$$

in which the numerical fluxes are now taken at time $(n+1)\Delta t$. After a linearization, this implicit scheme takes the form

$$(\mathcal{H} \Delta w)_{j,k} = \Delta w_{j,k}^{expl}, \tag{45}$$

where the right-hand side or *explicit stage* is given by (42)–(44) and $\mathcal{H}$ is the linear implicit operator.

Now we make two simplifications of the operator $\mathcal{H}$. First, we drop the approximation of the mixed second-order derivatives and then we replace the eigenvalues of Φ and Ψ by their upper bound in (34), i.e.,

$$\lambda_{\Phi}^{(i)} = \lambda_{\Psi}^{(i)} = 1.$$

Therefore, the matrices Φ and Ψ are both reduced to the identity matrix and

$$\mathcal{H} = I + \mathcal{H}_1 + \mathcal{H}_2, \tag{46}$$

with the 1-D difference operators $\mathcal{H}_1$ and $\mathcal{H}_2$ given by

$$\begin{aligned} \mathcal{H}_1 \Delta w &= \frac{\Delta t}{\delta x}\left[\mu_1(A_R \delta_1 \Delta w) - \frac{1}{2}\delta_1(|A_R|\delta_1 \Delta w)\right] \\ \mathcal{H}_2 \Delta w &= \frac{\Delta t}{\delta y}\left[\mu_2(B_R \delta_2 \Delta w) - \frac{1}{2}\delta_2(|B_R|\delta_2 \Delta w)\right]. \end{aligned} \tag{47}$$

The implicit stage (46) is then of Harten type [5]. It involves only three points by direction.

The implicit scheme (42)–(44), (45)–(47) has been shown to be always linearly stable. The implicit stage can be solved either by ADI factorization or by alternate line-relaxation of Jacobi or Gauss–Seidel type following the same lines as in [2] for the Lerat scheme. All these techniques lead to the solution of algebraic linear systems associated to block-tridiagonal matrices at each time iteration.

In practice, applying a line-relaxation technique allows the use of CFL numbers up to 1000 in our 2-D calculations. On the contrary, applying an ADI factorization yields convergence rate limitations as for many other schemes. The CFL numbers used here with the factored scheme are of the order of 10.

7. NUMERICAL APPLICATIONS

The present method is validated through the computation of various steady and slow unsteady compressible flows governed by the two-dimensional Euler equations

$$w_t + f(w)_x + g(w)_y = 0$$

with

$$w = \begin{bmatrix} \rho \\ \rho u \\ \rho v \\ \rho E \end{bmatrix}, \qquad F = \begin{bmatrix} \rho u \\ \rho u^2 + p \\ \rho uv \\ (\rho E + p)u \end{bmatrix}, \qquad G = \begin{bmatrix} \rho v \\ \rho uv \\ \rho v^2 + p \\ (\rho E + \rho)v \end{bmatrix},$$

where ρ is the density, p the pressure, u and v the Cartesian components of the fluid velocity, and E the specific total energy defined by

$$E = e + \frac{1}{2}(u^2 + v^2),$$

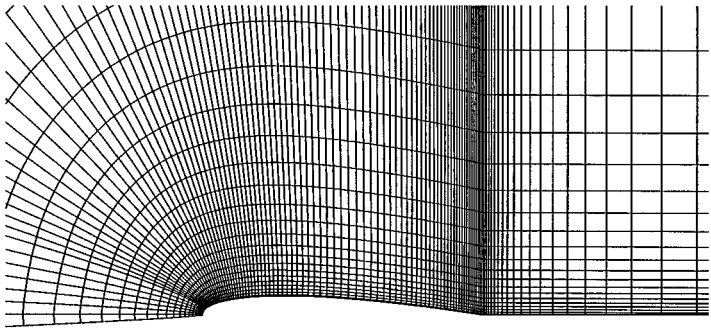

FIG. 3. The 124 × 32 mesh for the NACA0012 airfoil.

e being the specific internal energy. The pressure is related to ρ and e by the equation of state,

$$p = (\gamma - 1)\rho e$$

with $\gamma = 1.4$ in our calculations.

The scheme is applied on curvilinear meshes using a cell-centered finite-volume formulation. No limiter, entropy correction, or dissipative term is added to the present method.

7.1. *Transonic Flow over an Airfoil*

We first consider the steady transonic flow over the NACA0012 airfoil at Mach number 0.85 and zero angle of attack. The flow is symmetric and computed in the upper half domain on a C-mesh composed of 124 × 32 cells (see Fig. 3). On the airfoil, the slip condition is prescribed and the pressure is deduced from a conservative integral form of the momentum equation projected on the normal to the wall.

The computation starts from an uniform flow and is run with a local time-step associated with a constant and uniform CFL number. The convergence history of the present implicit method is shown in Fig. 4, using ADI factorization or line Gauss–Seidel relaxation (ALGS)

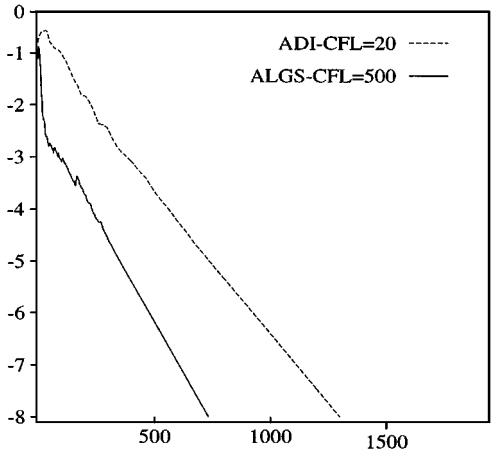

FIG. 4. Convergence histories for the transonic flow over the NACA0012 airfoil ($\log_{10}$ of the L_2-residual in terms of time-iterations).

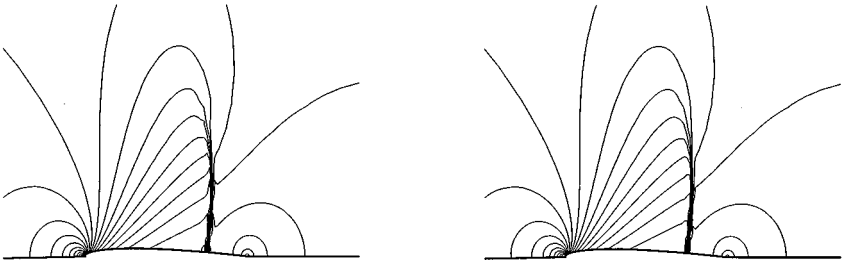

FIG. 5. Pressure contours, $\Delta p = 0.04$ (left, Lerat scheme; right, present scheme).

in the implicit stage. The L_2 residual is reduced by 6 orders of magnitude in about 1000 iterations with ADI (CFL $= 20$) and 500 iterations with ALGS (CFL $= 500$).

Concerning the steady numerical solutions, the pressure contours are shown in Fig. 5 and compared to those of the implicit Lerat scheme of Lax–Wendroff type. Both results are very similar, which confirms the second-order accuracy of the present method. Figure 6 compares the entropy contours of the two schemes and reveals a better behaviour for the present method. This is also apparent in Fig. 7 showing the solution on the airfoil, namely the pressure coefficient

$$C_p = \frac{p - p_\infty}{(1/2)\gamma p_\infty M_\infty^2}$$

and the entropy deviation

$$\Sigma = \frac{s - s_\infty}{s_\infty},$$

where $s = p/\rho^\gamma$ and the subscript ∞ refers to the freestream. The present scheme gives a lower entropy error upstream of the shock and a monotonic numerical shock profile over two mesh cells only.

Moreover, the present scheme has a steady solution that does not depend on the CFL number used in the convergence process, contrary to the Lerat scheme (see Figs. 8 and 9).

7.2. *Supersonic Flow over an Ellipse*

The second application concerns the supersonic flow over an ellipse of aspect-ratio 2.4 at Mach number 3 without incidence. This supersonic flow is computed over an half domain on the 32×32 mesh shown in Fig. 10.

The present scheme has been applied similarly as for the transonic flow problem, except that at inflow and outflow, supersonic boundary conditions are used. The numerical solution is shown in Figs. 11 and 12. The detached shock is well captured: it is sharp and non-oscillatory.

FIG. 6. Entropy contours, $\Delta s = 0.0005$ (left, Lerat scheme; right, present scheme).

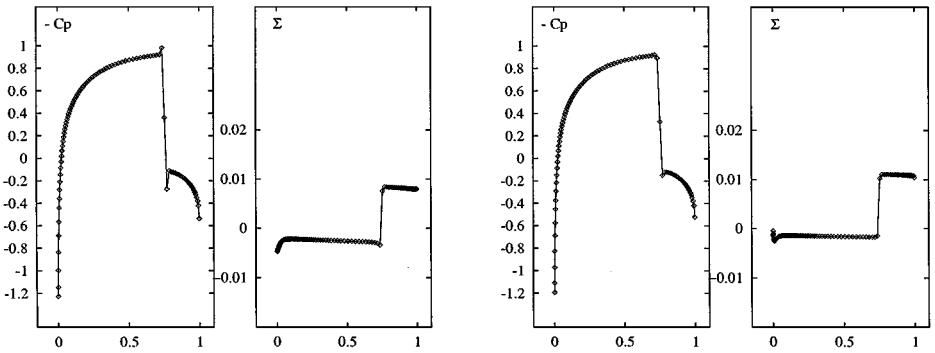

FIG. 7. Pressure coefficient and entropy deviation on the profile (left, Lerat scheme; right, present scheme).

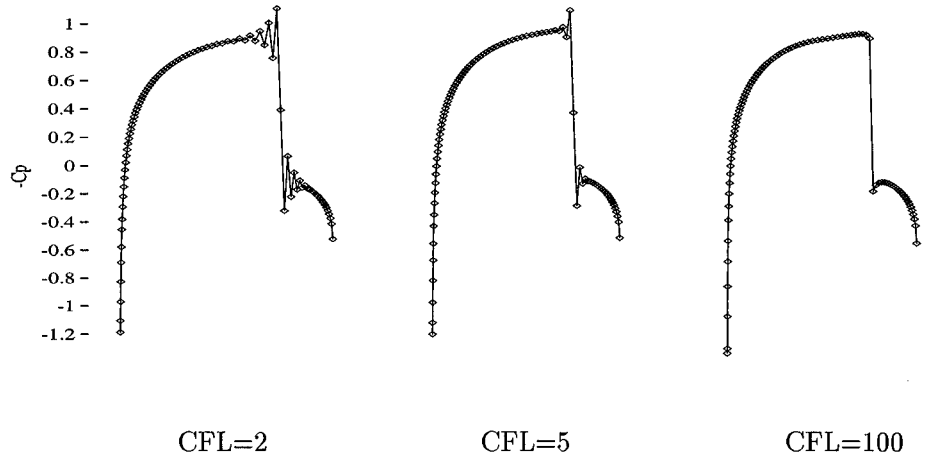

FIG. 8. Lerat scheme: shock profiles depend on the CFL numbers.

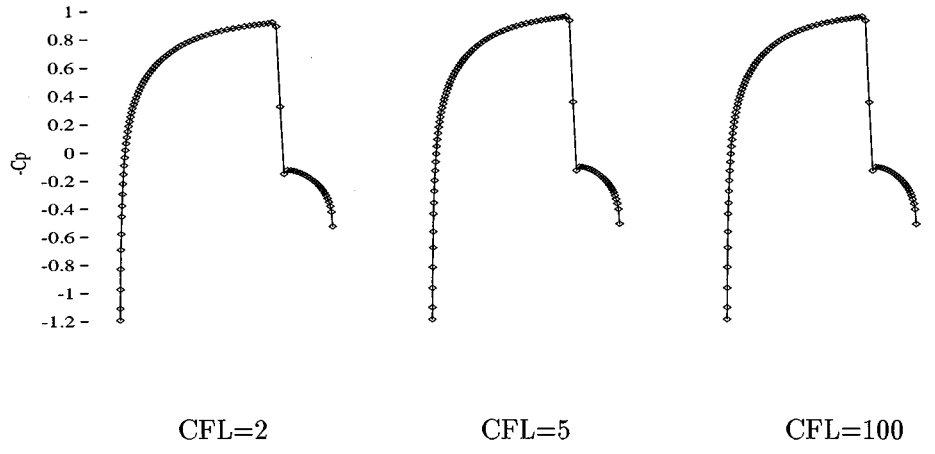

FIG. 9. Present scheme: shock profiles do not depend on the CFL numbers.

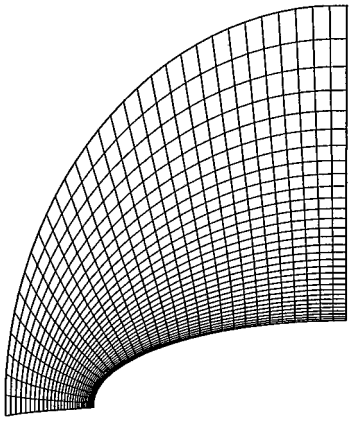

FIG. 10. The 32×32 mesh for the ellipse.

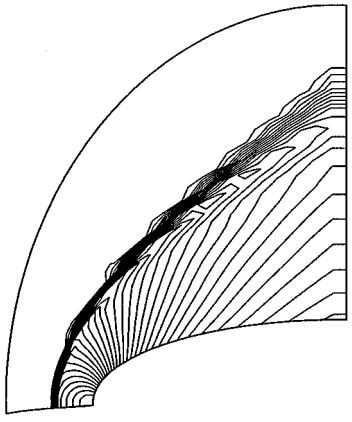

FIG. 11. Pressure contours, $\Delta p = 0.05$.

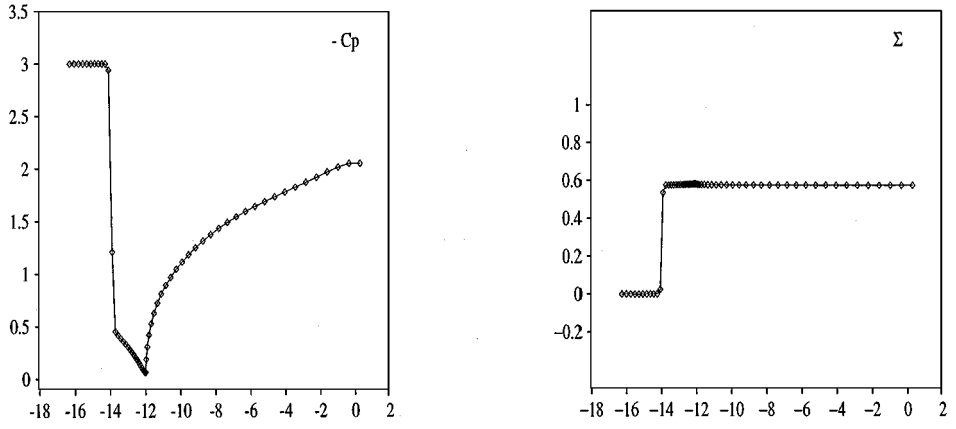

FIG. 12. Pressure coefficient and entropy deviation on the symmetry axis and the ellipse, $M_\infty = 3$.

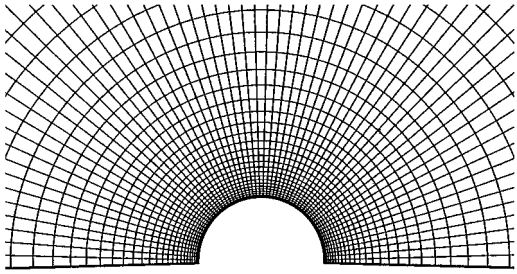

FIG. 13. The 64×32 mesh for the cylinder.

7.3. *Subsonic Flow over a Circular Cylinder*

We now consider a subsonic flow over a circular cylinder at Mach number 0.38. In these conditions, the maximal Mach number on the cylinder is slightly lower than one. The computational domain and the 64×32 mesh are shown in Fig. 13. The solution given by the present scheme is displayed in Figs. 14 and 15. The upstream/downstream symmetry is perfectly recovered and the entropy deviation is very low (smaller than 3×10^{-4}).

7.4. *Transonic Flow in a Compressor Cascade*

The present scheme has also been applied to internal flows in turbomachinaries. Here, we present a transonic flow calculation in the compressor cascade shown in Fig. 16. The computational domain is bounded by an inlet, an outlet, two blades, and four cut-lines on which periodicity conditions are prescribed. The mesh is composed of 120×30 cells.

At the inlet boundary, the Mach number is 1.301 and the incidence is about 63.4 degrees. At the outlet boundary, the pressure is prescribed. It is equal to 44% of the upstream stagnation pressure. On the two blades, the slip condition is enforced. The periodic boundary condition on the cut-lines is viewed as a matching condition between two subdomains and treated similarly as in [16].

Starting from an uniform flow, the convergence history of the present method is shown in Fig. 17, using ADI factorization or ALGS relaxation in the implicit stage. The L_2 residual

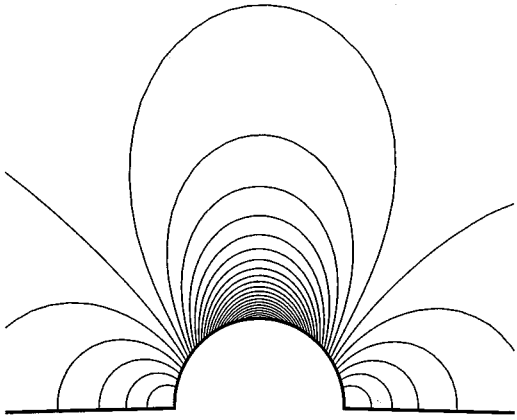

FIG. 14. Pressure contours, $\Delta p = 0.02$.

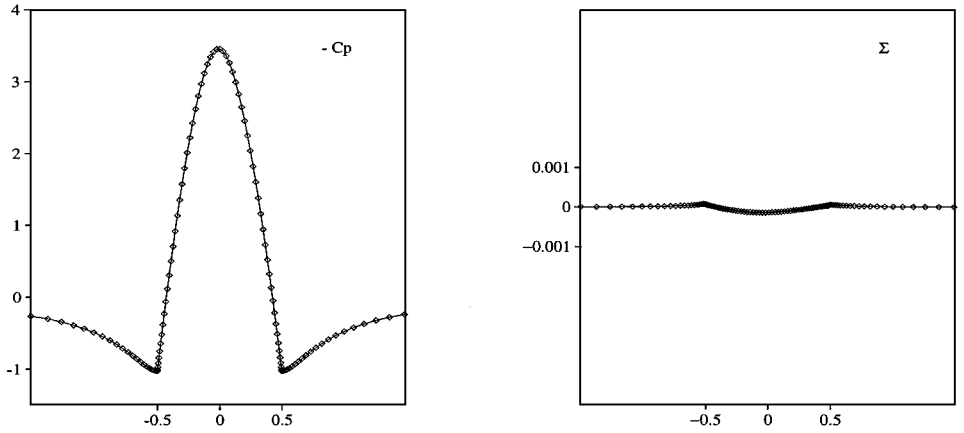

FIG. 15. Pressure coefficient and entropy deviation on the symmetry axis and the cylinder, $M_\infty = 0.38$.

is reduced by 6 orders of magnitude in about 1600 iterations with ADI (CFL = 10) and only 70 iterations with ALGS (CFL = 1000). To reach this residual, the CPU time for the relaxed method is about 16.4 seconds on a CRAY J916 computer, which is nearly ten times less than with the factored method.

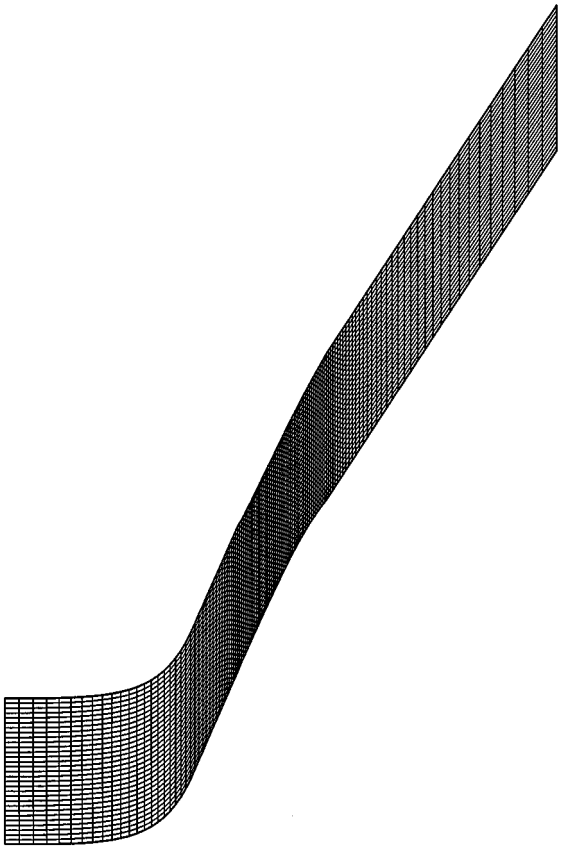

FIG. 16. The 120 × 30 mesh for the compressor cascade.

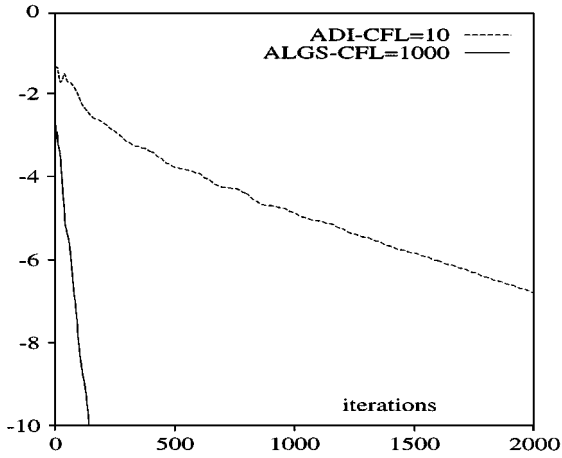

FIG. 17. Convergence histories for the compressor cascade.

The Mach number contours are presented in Fig. 18 and compared to those obtained by a first-order upwind scheme [20] on the same mesh, also using 3 points per space direction. Owing to its real second-order accuracy, the present scheme gives a much better resolution of the main features of the flow: the weak compression around the leading edge, the λ-shock, and the skewed slip line.

7.5. *Slow Unsteady Flow around a Moving Airfoil*

We finally consider a slow unsteady problem, that is, the flow over the NACA0012 airfoil in plane motion of great amplitude. The freestream Mach number is 0.536 and there is no incidence. The airfoil moves in the horizontal direction at the speed

$$u_0 = -M_0 a_\infty \sin kt, \tag{48}$$

where $M_0 = 0.327$, $k = 0.185$ (reduced frequency), and a_∞ denotes the freestream sound speed. This is a 2-D simulation of the flow conditions over a section of a helicopter rotor blade near the tip of the blade, studied by Lerat and Sides in 1979 [13]. The Mach number relative to the airfoil has the time-evolution

$$M_{r,\infty} = M_\infty + M_0 \sin kt.$$

During the first half-cycle of the periodic evolution (blade forward motion), the relative Mach number goes from 0.536 up to 0.863 and down again to 0.536. This yields the formation of a shock wave travelling first downstream, then rapidly upstream and vanishing before reaching the leading edge. During the second half-cycle, $M_{r,\infty}$ remains lower than 0.536 and the flow regime is subsonic.

This unsteady problem is solved on a 94×24 mesh moving with the airfoil (see Fig. 19). The Euler equations are written in a frame attached to the mesh but still use the components of the fluid absolute velocity in the absolute frame, i.e.,

$$w_t + [f(w) - u_0 w]_x + g(w)_y = 0,$$

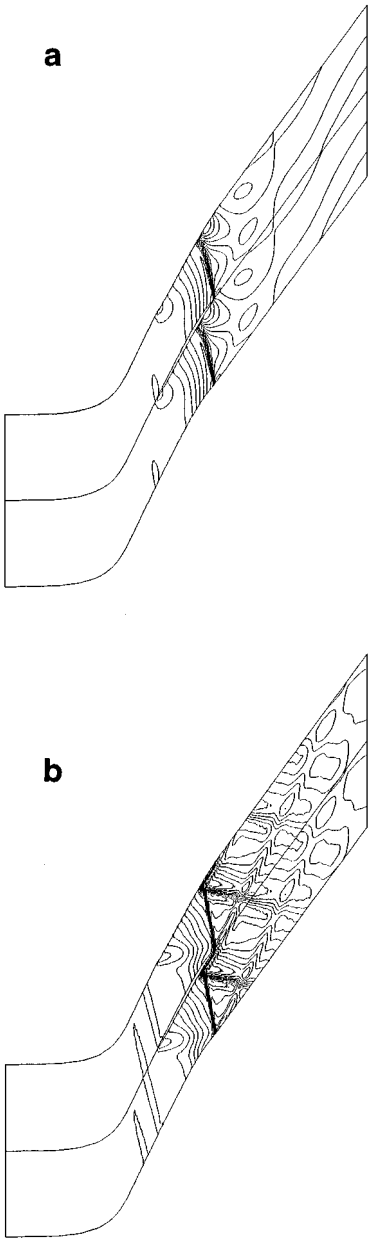

FIG. 18. Mach number contours ($\Delta M = 0.05$) in the compressor cascade. (a) First-order upwind scheme. (b) Present 3×3-point scheme.

where w, $f(w)$, and $g(w)$ are defined as previously. The slip boundary condition on the moving airfoil takes the form

$$(\mathbf{V} - \mathbf{V}_0) \cdot \mathbf{n} = 0,$$

where $\mathbf{V}$ is the fluid absolute velocity, $\mathbf{V}_0 = (u_0, 0)^T$, and $\mathbf{n}$ is a normal to the airfoil. For this unsteady flow calculation, a conservative treatment in time is necessary. This is not the case for the implicit stage (45)–(47) because of the term $\mu_1(A_R \delta_1 \cdot)$ in the difference operator

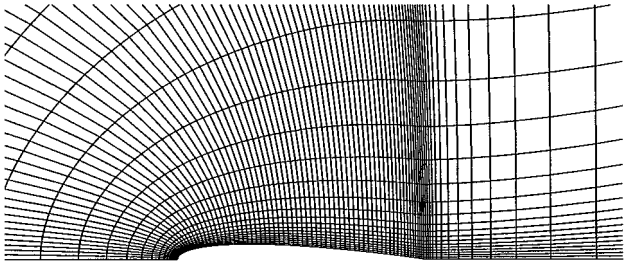

FIG. 19. The 94×24 mesh for the moving NACA0012 airfoil.

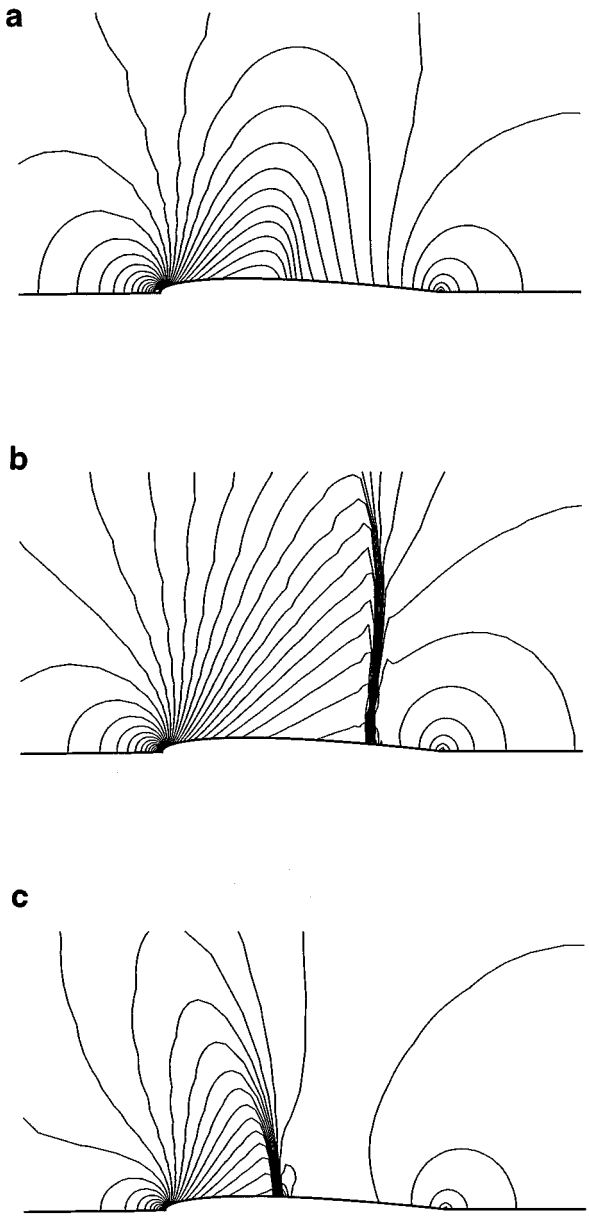

FIG. 20. Pressure contours around the moving airfoil ($\Delta p = 0.075$) calculated with CFL $= 12$. (a) $kt = 60^\circ$ ($M_{r,\infty} = 0.819$). (b) $kt = 120^\circ$ ($M_{r,\infty} = 0.819$). (c) $kt = 150^\circ$ ($M_{r,\infty} = 0.699$).

$\mathcal{H}_1$ and $\mu_2(B_R\delta_2\cdot)$ in $\mathcal{H}_2$. To restore conservation, we replace these terms by $\delta_1(A_R\mu_1\cdot)$ and $\delta_2(B_R\mu_2\cdot)$, respectively, which does not modify the linear properties of the scheme.

The initial condition corresponds to a steady flow over the airfoil at $M_\infty = 0.536$ and the solution is advanced using an uniform time-step ($\mathrm{CFL}_{\max} = 12$). Figure 20 shows the isobar lines calculated at the times $kt = 60^\circ$, 120°, and 150° during the first period. Note that the first two instants give the same relative Mach number ($M_{r,\infty} = 0.819$); nevertheless the flow is subsonic for $kt = 60^\circ$ and transonic for $kt = 120^\circ$. The formation and the excursion of the shock wave are well represented by the present method and there is no excessive dissipation even though the formal order of accuracy in time is only one.

8. CONCLUSIONS

An very simple multidimensional upwind scheme has been proposed for solving the Euler equations. It is deduced from the Lax–Wendroff type approximation by introducing some matricial time-step. Involving 3×3 points only in two-dimension, the scheme is truly second-order accurate at steady state and very close to a genuinely multidimensional upwind method.

Owing to an efficient implicit treatment, the present scheme allows the use of large CFL numbers and converges quickly to the steady solutions. For various 2-D aerodynamic problems, the scheme has produced accurate non-oscillatory solutions without any correction. Numerical shock profiles are sharp even if they are not aligned with the mesh lines. The extension of the method to viscous flow problems is in progress.

ACKNOWLEDGMENT

The authors thank SNECMA for supporting this research.

REFERENCES

1. Ph. Colella, Multidimensional upwind methods for hyperbolic conservation laws, *J. Comput. Phys.* **87**, 171 (1990).
2. C. Corre, K. Khalfallah, and A. Lerat, Line-relaxation methods for a class of centred schemes, *Comput. Fluid Dynam. J.* **5**, 213 (1996).
3. M. Fey and R. Jeltsch, A simple multidimensional Euler scheme, in *Computational Fluid Dynamics'92*, edited by Ch. Hirsch *et al.* (Elsevier, Amsterdam, 1992), p. 45.
4. A. Harten, High resolution schemes for hyperbolic conservation laws, *J. Comput. Phys.* **49**, 357 (1983).
5. A. Harten, On a class of high resolution total-variation stable finite-difference schemes, *SIAM J. Numer. Anal.* **21**, 4 (1984).
6. Ch. Hirsch, C. Lacor, and H. Deconinck, Convection algorithms based on a diagonalisation procedure for the multidimensional Euler equations, *AIAA Paper* 87-1163, June 1987.
7. C. Hirsch and P. V. Ransbeeck, Multidimensional upwinding and artificial dissipation, in *Frontiers of Computational Fluid Dynamics*, edited by D. A. Caughey and M. Hafez (Wiley, New York, 1994), p. 597.
8. Y. Huang, K. Khalfallah, and A. Lerat, A second-order upwind scheme without limiter for steady Euler equations, in *Computational Fluid Dynamics'94*, edited by S. Wagner *et al.* (Wiley, New York, 1994), p. 587.
9. P. D. Lax and B. Wendroff, Systems of conservation laws, *Comm. Pure Appl. Math.* **13**, 217 (1960).
10. A. Lerat, Une classe de schemas aux differences implicites pour les systemes hyperboliques de lois de conservation, *C. R. Acad. Sci. Paris A* **288**, 1033 (1979).
11. A. Lerat, Implicit methods of second order accuracy for Euler equations, *AIAA J.* **23**, 33 (1985).

12. A. Lerat, Multidimensional centred schemes of the Lax–Wendroff type, in *Computational Fluid Dynamics Review 1995*, edited by M. Hafez and K. Oshima (Wiley, New York, 1995), p. 124.
13. A. Lerat and J. Sides, Simulation of unsteady transonic flow using the Euler equations in integral form, *Israel J. Technol.* **17**, 302 (1979).
14. A. Lerat and J. Sides, Efficient solution of the steady Euler equations with a centered implicit method, in *Numerical Methods for Fluid Dynamics 3*, edited by K. W. Morton and M. J. Baines (Clarendon, Oxford, 1988), p. 65.
15. A. Lerat, J. Sides, and V. Daru, An implicit finite-volume method for solving the Euler equations, in *Lecture Notes in Physics* (Springer-Verlag, New York/Berlin, 1982), Vol.170, p. 343.
16. A. Lerat and Z. N. Wu, Stable conservative multidomain treatments for implicit Euler solvers, *J. Comput. Phys.* **123**, 45 (1996).
17. D. W. Levy, K. G. Powell, and B. Van Leer, Use of a rotated Riemann solver for the two-dimensional Euler equations, *J. Comput. Phys.* **106**, 201 (1993).
18. K. W. Morton, M. A. Rudgyard, and G. J. Shaw, Upwind iteration methods for the cell vertex scheme in one dimension, *J. Comput. Phys.* **114**, 209 (1994).
19. K. G. Powell and B. Van Leer, Tailoring explicit-marching schemes to improve convergence characteristics, in *Von Karman Institute for Fluid Dynamics Lecture Series* (Bruxelles, 1990), Vol. 1990-03.
20. P. L. Roe, Approximate Riemann solvers, parameter vectors, and difference schemes, *J. Comput. Phys.* **43**, 357 (1981).
21. P. L. Roe, A basis for upwind differencing of the two-dimensional unsteady Euler equation, *J. Comput. Phys.* **63**, 458 (1986).
22. P. K. Sweby, High resolution schemes using flux limiters for hyperbolic conservation laws, *SIAM J. Numer. Anal.* **21**, 4 (1984).
23. B. Van Leer, Towards the ultimate conservative difference scheme. V. A second order sequel to Godunov's method, *J. Comput. Phys.* **32**, 101 (1979).